JPET #107847

Identification of Cell Adhesion Molecules in the Human Follicle Associated Epithelium (FAE) that improve Nanoparticle Uptake into the Peyer's patches

Elisabet Gullberg, Åsa V Keita, Sa'ad Y Salim, Margaretha Andersson, Karin D Caldwell, Johan D Söderholm and Per Artursson

Department of Pharmacy, Uppsala University, SE-751 23 Uppsala, Sweden (EG, PA); Department of Biomedicine and Surgery, Linköping University, Faculty of Health Sciences, SE-581 85 Linköping, Sweden (EG, ÅVK, SYS, JDS); Department of Surface Biotechnology, Uppsala University, SE-751 23 Uppsala, Sweden (MA, KDC).

1

JPET #107847

Running title: Nanoparticle targeting to human Peyer's patches

Corresponding author: Professor Per Artursson, Dept. Pharmacy, Box 580, BMC, SE-751

23 Uppsala Sweden, Phone: +46-18-471 4471, Fax: +46-18-471 42 23, E-mail:

Per.Artursson@farmaci.uu.se

Number of text pages: 19 (not including abstract and figure legends)

Number of tables: 0

Number of figures: 8

Number of references: 40

Abstract: 250 words

Introduction: 742 words

Discussion: 1283 words

Abbreviations: FAE; Follicle Associated Epithelium, HBSS; Hank's balanced Salt Solution,

PP; Peyer's Patches, VE; Villus Epithelium; VED; Villus Epithelium adjacent to Dome.

Recommended section assignment: Absorption, Distribution

JPET #107847

Abstract

The aim of this study was to identify cell adhesion molecules that could serve as targets of the human follicle associated epithelium (FAE) overlying Peyer's patches and to assess nanoparticle uptake levels across this epithelium. We first studied the expression of the mouse M-cell marker β_1-integrin and used a model of human FAE derived from intestinal epithelial Caco-2 cells and Raji B-cells to identify additional potential targets by cDNA-array. The protein expression of potential targets in the model FAE and in human ileal FAE tissues was quantified by immunofluorescence. Integrin targeting was studied by investigating the transport of RGD-coated (integrin-binding), RGE-coated (non-integrin-binding) and uncoated nanoparticles across ileal specimens mounted in Ussing chambers. Both β_1-integrin and the cell adhesion molecule CD9 were more abundantly expressed in the model and human FAE compared with the Caco-2 control cells or villus epithelium (VE). Uncoated nanoparticles were not taken up across either FAE or VE. General integrin targeting with RGD improved the nanoparticle transport dramatically across the FAE and to a lower extent across the VE. Compared with RGE, RGD improved transport four-fold across the FAE. There was no difference in the transport of RGD- and RGE-coated nanoparticles across the VE. In conclusion, β_1-integrin and CD9 were identified as targets in human FAE. The difference in RGD- and RGE-mediated transport across the FAE, but not the VE, suggest that a specific integrin interaction was the dominating mechanism for improved nanoparticle uptake across the FAE., while charge interaction contributed substantially to the improved VE uptake.

Introduction

Oral delivery of antigens is by far the most effective method of inducing gastrointestinal mucosal immune responses (O'Hagan and Rappuoli, 2006). There are promising data from animal studies using micro-particulate carriers for delivery of subunit antigens, but so far, few of these have succeeded in inducing effective immune responses in humans (Mutwiri et al., 2005). It is therefore being increasingly questioned whether encapsulated antigens can be taken up in sufficient quantities to induce adequate immune responses. Studies of commonly used biogradable particles (PLGA) have shown that less than 0.01% of the given dose is taken up of into human cell cultures or animal tissues (Brayden, 2001). These data suggest that an improvement in the efficacy of particle uptake is required, before subunit oral vaccination becomes a feasible option. In this perspective, surprisingly little is known of particle uptake in the human intestine.

Targeting to specific surface receptors on epithelial cells by use of receptor ligands on the particle surface has been successful in improving uptake of proteins across intestinal epithelial cells in culture (Russell-Jones, 2004). However *in vivo*, the mucus layer most likely limits particle uptake across the human villus epithelium (VE). In contrast, antigen uptake across the follicle-associated epithelium (FAE), covering Peyer´s patches (PP), is facilitated by the absence of mucus-producing Goblet cells and a reduced expression of hydrolases. A prominent feature of this epithelium is also the presence of specialized M-cells (Owen, 1999) that transport intact protein antigens, as well as particles, viruses and bacteria across the epithelial cell layer (Owen 1999; Neutra, 1999). We have recently shown an increased transport of antigens and bacteria across the human FAE compared with the VE (Keita et al., 2006).

Thus, the FAE and M-cells are prime targets when aiming at improved particle uptake and immune responses. Targeting of particles to mouse M-cells by use of various ligands,

including Ulex Europeaus Agglutinin 1 (UEA-1; Foster et al., 1998) and immunoglobulins (Smith et al., 1995), increased adherence and transcytosis of particles across M-cells. However, the magnitude of these effects has not been assessed and the size of the particulate carrier and accessibility of the receptor seem critical for the outcome (Mantis e al., 2000; van der Lubben et al., 2001)

In humans, little is known about surface proteins that could act as specific targets in human FAE. Lectins such as the *Sambucus Nigra Antigen* (SNA) appear to predominantly stain polysaccharides in the human FAE (Jepson et al., 1996), but the expression of these sugar moities varies considerably along the intestine, as well as among individuals (Gebert et al., 1996; Sharma et al., 1996). Two putative human M-cell markers have been reported; Cathepsin E (Finzi et al., 1992) and the Sialyl Lewis A Antigen (Giannasca et al., 1999), but unfortunately, these results could not be reproduced (Wong et al., 2003). mRNA-transcripts coding for Claudin-4 and the cell adhesion protein TM4SF3 seem specific to the human FAE, but it is not known if the corresponding proteins are accessible for targeting (Lo et al., 2004).

β_1-integrin, on the other hand, marks the surface of mouse M-cells and mediates uptake of bacteria – alone or in complex with α_5-integrin (Clark et al., 1998; Tyrer et al., 2006). Both we and others have also demonstrated an increased apical expression of β_1-integrin in model FAE cell monolayers (Schulte et al., 2000, des Rieux et al., 2005). Studies in rats have suggested that targeting of particles to β_1-integrin may improve uptake across the intestinal epithelium, although these data were inconclusive regarding site of uptake (Hussain and Florence, 1998). Surprisingly, the expression of β_1-integrin has not yet been reported in human FAE and the effect of targeting particles to β_1-integrin has not been investigated in human or mouse intestine.

The aim of this study was to identify cell adhesion molecules that could serve as targets in the human FAE. We first selected β_1-integrin and then identified additional molecules unique to

the human FAE, using a specific cell adhesion/cell interaction cDNA array. Since it was impossible to isolate sufficient quantities of pure and viable epithelial cells from human FAE, we initially used a modification of an established human co-culture model of the FAE, which has several phenotypic features of tissue FAE (Kerneís et al., 1997, Gullberg et al., 2000). The protein expression of β_1-integrin and the other targets identified on the array was assessed in the model and in human ileal FAE. Finally, we explored these findings for improved uptake of nanoparticles across human FAE.

Methods

Cell culture

Caco-2 cells (ECACC, Salisbury, UK), Clone 1 Caco-2 cells (Dr. Maria Rescigno, University of Milano-Bicocca, Milano, Italy) and the human Burkitt's lymphoma cell line Raji (ATCC, ML, U.S.A.) were maintained as described previously (Gullberg et al.., 2000). For both RNA isolation and transport experiments, Caco-2 cells were grown on polycarbonate filters (pore size: 3.0 µm, Costar, Baedvenhorp, NL), which were coated with Matrigel™ (Becton Dickinson, U.S.A). To obtain the model FAE, $5x10^5$ Raji cells were added to the basolateral chamber of the Caco-2 cell monolayers at day 14. The co-cultures were maintained for 4-5 days (Gullberg et al., 2000). Mono-cultures of Caco-2 cells grown on filters for 18-19 days were used as controls. The transport of fluorescence-labelled polystyrene particles (0.5 µm, Invitrogen, the Netherlands) was use to verify the function of each batch of model FAE. Transepithelial electrical resistance (TEER) was used for assessment of cell monolayer integrity (see transport experiments below). The cell monolayers were prepared for immunofluorescence studies by 10 minutes fixation in 4% buffered formaldehyde and subsequent rinsing with Hank's balanced salt solution (HBSS with calcium, magnesium and sodium bicarbonate, Invitrogen). They were stored in HBSS until use.

JPET #107847

RNA isolation, array hybridization and gene expression analysis

For RNA isolation, the cell monolayers were rinsed several times with ice-cold Phosphate buffered Saline (PBS, 0.01M NaPO$_4$, 0.14 M NaCl, 0.003M KCl) and scraped off the filters into RNAse-inhibiting Denaturing Solution™ (Ambion, Austin, TX, U.S.A). Total RNA was isolated with Ambion's Totally RNA kit (Ambion, Austin, TX, U.S.A.) according to the manufacturer's instructions. All RNA samples were DNAse-treated and control PCR was run on all RNA samples to confirm that they were free from genomic DNA. RNA samples from 3 pooled model FAE and Caco-2 cell batches (6 filters in total) were reversibly transcribed to ^{32}P-cDNA and hybridised to Clontech™ cell-adhesion/cell-interaction arrays (Clontech, CA, U.S.A), according to the manufacturer's instructions. The primer mix used for reverse transcription only amplified transcripts from genes present on the array.

Differences in gene expression were analyzed by Atlas Image™ (Clontech, CA, U.S.A). Signals lower than the average background signal were filtered out. To compare two or more arrays, the signal intensities of all genes on the arrays were normalized according to the manufacturers instructions.

Isolation of Peyer´s patches from human ileum and preparation of cryosections

The study was approved by the local committee of human ethics in Linköping and all subjects gave their informed consent. Specimens were obtained from the ileum next to the ileocaecal valve during ileo-colonic surgery of eight patients diagnosed with colon cancer, at the University Hospital of Linköping. The median age of the patients (5 men and 3 women) was 67 years (range 35-87). Immediately following dissection, the specimens were placed in ice-cold oxygenated Krebs Ringer buffer (115 mM NaCl, 25 mM NaHCO$_3$, 2mM K$_2$HPO$_4$, 1,25 mM CaCl$_2$, 1,2 mM MgCl$_2$), pH 7.4 and taken to the laboratory for the experiments. A pathologist examined the specimens, which all showed macroscopically normal histology. While still immersed in ice-cold buffer, the external muscle and myenteric plexus were

7

stripped from the surgical specimens. After identification in a dissection microscope, transilluminated from below (Keita et al., 2006), regions of VE and FAE were cut out, oriented to give cross sections of the intestinal wall, snap frozen in liquid nitrogen and mounted in Cryomount. Cryosections (5μm) were cut using a microtome (Leica, Germany) and dried at room temperature on glass slides over night, before storage at –70ºC. Sections were prepared for immunofluorescence by fixing in ice-cold acetone for 10 minutes, followed by drying at room temperature.

Immuno-staining of fixed cell cultures and cryosections

All cryosections and formaldehyde-fixed cell cultures were micro-waved for 10 minutes in 10 mM citrate, pH 6 (β_1-integrin) or 1 mM EDTA, pH 8 (CD9) as recommended by the manufacturers of the antibodies. After cooling to room temperature, the sections/cells were rinsed several times with distilled water, washed in HBSS and permeated with 0.2% Triton-X-100 for 5 minutes (β_1-integrin), or with Cryofix (Merck, Germany) for 2 minutes (CD9). After blocking with HBSS containing 1% fetal calf serum, the sections/cells were stained with primary antibodies to β_1-integrin (clone J10, 400 □g/ml, Biogenex, CA, U.S.A.) or CD9 (clone 72F6, 1:100, Serotec, Oxford, UK). The primary antibodies were detected with secondary goat-anti-mouse IgG1 antibodies conjugated to Alexa 488 (Molecular Probes/Invitrogen, the Netherlands). Antibodies to CD20 (clone L26, 1:100, Biomeda, CA, U.S.A.) were used to visualize CD20-positive B-cells in lymphoid follicles and M-cells (Yamanaka et al., 2001). CD20 was detected using Alexa568 goat-anti-mouse IgG2a (Molecular Probes/Invitrogen, the Netherlands). Cells/sections incubated with isotype-matched antibodies were used as controls.

Immunofluorescence analysis of cell cultures and human tissue

The immuno-fluorescence of β_1-integrin and CD9 in cell cultures were analyzed by optical sectioning in a Confocal Laser Scanning Microscope (CLSM, Leica, Germany), using the same settings for the model FAE and Caco-2 epithelium. Fluorescence intensity profiles were made in ImageJ software (rsb.info.nih.gov/ij). The human tissue sections were analyzed using an Axioplan fluorescence microscope (Zeiss, Germany). Pictures were captured with a CCD-camera (Hamamatsu C4542-95B, Japan), using the same gain and exposure times for all sections on the same slide. Relative fluorecence intensities of the epithelium were measured using ImageJ software. Two slides were prepared on different occasions for each protein and each patient. Four to eight sections, representing 2-3 different cell layers, were analyzed per patient. In each tissue section, all types of epithelia, FAE, VE and VED (villus epithelium adjacent to dome), were represented and their fluorescence intensities relative each other was determined within the same section. Ten measurements of cell membrane fluorescence intensities were performed on equal areas of the different type of epithelia in each section. Background values obtained from control sections on each slide, were subtracted from the true measured fluorescence intensities found on the same slide. The data were normalized to compare protein expression among the patients. The fluorescence intensity for each sample from a particular patient was divided by the sum of the fluorescence intensities of the total tissue sections for that patient. By two-way ANOVA, we analyzed the difference in fluorescence intensities between each type of epithelia from the same patient, and in each type of epithelia between different patients. The tissue obtained from two patients lacked villus epithelium. For these patients, only the fluorescence intensities of FAE and VED are reported.

Preparation of RGD-and RGE-coated polystyrene nanoparticles

Yellow-green fluorescent polystyrene particles (average diameter 200 nm) were purchased from Polysciences Inc. (Warrington, PA). Pluronic F108 modified with a thiol-specific

pyridyl disulphide group (Cell Link) was kindly donated by Allvio Inc. (Lake Forest, CA). Two polypeptides containing the RGD motif (Cys-Gly-Arg-Gly-Asp-Ser-Tyr) and the RGE motif (Cys-Gly-Arg-Gly-Glu-Ser-Tyr) were synthesized at the Department of Medicinal Chemistry, Uppsala University. The Pluronic surfactant was adsorbed onto the particles by a hydrophobic interaction and the peptide was subsequently attached to the hydrophilic parts of the linker using the cysteine residue. The reaction was confirmed by measuring the UV absorbance at 343 nm from released pyridyl disulphide groups. A Shimadzu UV-2102 PC UV-VIS scanning spectrophotometer was used and the extinction coefficient at the wavelength was 8080 $M^{-1}cm^{-1}$. The preparation, purification and characterization procedures are described in detail elsewhere (Andersson et al., 2005).

Transport of nanoparticles across the model FAE and Caco-2 epithelium

Transport experiments were performed in HBSS at pH 7.4. After washing and equilibration in HBSS/fetal calf serum at 37ºC for 30 minutes, the transepithelial electrical resistance (TEER) of the cell monolayers was measured. Cell monolayers with a TEER above 175 $\Omega*cm^2$ were included in the experiments. 2.5 x 10^9 yellow-green fluorescent polystyrene particles, coated with RGD or RGE were added to the apical side. For the inhibition experiments, the cell monolayers were preincubated apically with 0.5 mM RGD-peptide (H-Arg-Gly-Asp-OH; Bachem, Germany) for 1 hour at room temperature before adding the particles. Samples were collected after 1 hour and analyzed in a Fluorescence Activated Cell Scan (FACS, Becton Dickinson, MA, U.S.A). Analysis of transport data was performed using one-way ANOVA and t-tests.

Uptake and transport of RGD-coated particles across human FAE and VE

Sections of VE and FAE, identified microscopically as described above, were cut to appropriate sizes and mounted in modified Ussing chambers (Harvard apparatus Inc.,

Holliston, MA, USA). FAE segments were carefully adjusted so that the patches covered the entire exposed tissue surface area (4.9 mm^2). The transport experiments were performed in Krebs Ringer buffer (see above for composition), pH 7.4, 37ºC, with the addition of 10 mM mannitol on the mucosal side and 10 mM glucose on the serosal side of the segments. The segments were continuously oxygenated by circulating 95% O_2 / 5% CO_2 gas and equilibrated for 40 min to achieve steady-state conditions. The integrity and viability was continuously monitored by measuring the TEER, short-circuit current and resting potential of the segments (Keita et al., 2006). Only segments that stabilized with a resting potential of less than -0.5 mV were included in the experiments. During inhibition experiments, 0.5 mM RGD-peptide (see above) was added to the mucosal side of the specimens 1 hour before adding the particles. Approximately, 2.5 x 10^9 particles/ml, with or without RGD- and RGE-coating were added to the mucosal side of the tissue (particles without peptide carried only adsorbed Pluronic linker). After 2 hours, the serosal buffer was withdrawn and the number of particles was measured by FACS. Analysis of transport data was performed using one-way ANOVA and t-tests. For qualitative assessment of particle uptake, the tissues were washed with PBS (composition, see above) to remove excess particles after 15 and 45 minutes and the specimens were fixed with 4% formaldehyde overnight. Subsequently, the tissues were rinsed with PBS, labeled with 22 nM phalloidin-Alexa Fluor 594 (Molecular Probes/Invitrogen, The Netherlands) for 30 minutes, washed repeatedly with PBS and the whole tissue was visualized in PBS-containing chambers under a Nikon Eclipse E600W confocal laser scanning microscope (Nikon, NY, USA).

Results

Increased expression of β_1-integrin in human FAE

Immuno-fluorescent staining of β_1-integrin in human Peyer's patches, revealed increased expression of β_1-integrin in human FAE compared with the surrounding villi. In the FAE, β_1-integrin was strongly expressed all around the basolateral face of the epithelial cells (Fig. 1A and B). β_1-integrin expression could also be found on the apical surface of the FAE, typically where CD20-positive cells infiltrated the epithelium (Fig 1D and F), but occasionally also in epithelial cells not associated with CD20-positive lymphocytes (Fig 1E). In contrast, β_1-integrin predominantly lined the basal part of the epithelial cells of the surrounding villi and was strongly expressed on cells in the lamina propria. This expression pattern compares well with previous studies on β_1-integrin expression in human intestinal villi (Lussier et al., 2000). Thus, it seemed that β_1-integrin had an increased accessibility in human FAE and was indeed a promising target. The next step was to identify additional targets by cDNA array, using our previously established model FAE.

Increased gene expression of adhesion and actin-associated proteins in the model FAE

There were differences in the expression of 18 (7%) of the 256 genes represented on the cell adhesion/cell interaction array between the model FAE and the Caco-2 epithelium. These genes code for proteins involved in cell adhesion, epithelial cell polarity and differentiation, actin dynamics and extracellular matrix remodeling (Fig. 2). In particular, the expression of cell adhesion molecules CD9, CD4, α_5-integrin (ITGA5) and epithelial differentiation markers Plakoglobin (PKGB), Desmoplakin II/III (DSP) and Wnt-5a was induced in the model FAE. The expression of E-cadherin (CDHE) was down-regulated. Among the genes coding for proteins involved in extracellular matrix remodeling, two matrix metalloproteinases, MMP14 and MMP17, were induced. In agreement with a previous study, we did not find an

upregulation of β_1-integrin transcripts in the model FAE. Hamzaoui et al. (2004) nicely demonstrated that an increased expression of β_1-integrin in the apical membrane of FAE-like cell monolayers was due to increased maturation of existing precursors, rather than an increase in production of the protein per se.

Assessing the protein expression of all the genes identified by the array was beyond the scope of this study. The cell adhesion molecules CD9 and CD4 were chosen for further investigation, since they exhibited the most pronounced upregulation in expression and since both of these proteins have been reported to act as co-receptors for viruses and bacteria. CD9 is a tetraspan protein that interacts with integrins in the cell membrane (Berditchevski et al., 1997) and CD4 is a well-known co-receptor for HIV (Dalgleish et al., 1984). We therefore compared the expression of these two proteins with the expression of β_1-integrin in the model FAE.

Enhanced protein expression of CD9 in the model FAE compared with the Caco-2 epithelium

The protein expression of CD9 was clearly enhanced in the model FAE compared with the Caco-2 epithelium (Fig. 3A-B). In both epithelia, CD9 was expressed laterally; however, expression in the basal and apical cell membranes was most pronounced in the model FAE. We were unable to find protein expression of CD4 in any of the two epithelia (Fig 3C-D). RT-PCR studies revealed that there were no difference in the number of CD4 transcripts between the model FAE and Caco-2 control epithelium (data not shown). Thus, the increase in CD4 gene expression was falsely detected by the cDNA array. In contrast, the increase in CD9 expression was confirmed by RT-PCR, with a ratio of 1.5 CD9 mRNA transcripts in the model FAE compared with the Caco-2 epithelium.

13

The expression of β_1-integrin was evenly distributed in the Caco-2 cells, but in the model FAE it was highly expressed in the apical membrane (Fig 3E-F), as previously reported (des Rieux et al., 2005).

Next, we analyzed the expression of CD9 in human Peyer´s patches and assessed the expression levels of both CD9 and β_1-integrin in different individuals.

The expression of both β_1-integrin and CD9 is higher in human FAE than in villus epithelium

Qualitative assessment of CD9 expression in human Peyer's patches, revealed that the FAE was indeed positive for CD9, while the VE was negative (Fig. 4A). In addition, CD9 was expressed by cells in the lamina propria in all specimens and could also be found in the lymphoid follicles. The expression of CD9 in VE is in agreement with a previous study of CD9 expression in the human small intestine (Sincock et al., 1997). In concordance with the results obtained in cell cultures, CD9 expression was found in both the apical and basolateral membranes of the epithelial cells in the FAE (Fig 4B).

Semiquantitative assessment of the expression levels of β_1-integrin and CD9 in the 8 individuals studied, confirmed our qualitative findings (Fig. 5). The expression levels of both proteins were 2-3-fold higher in the FAE than in the VE. In several of the specimens obtained, the villi adjacent to the dome (Fig. 5A, VED) also expressed CD9, while villi situated further away from the dome (VE) displayed no or low expression (Fig. 5B). In contrast, there was no difference in β_1-integrin expression between the VED and VE (Fig. 5C).

Increased transport of integrin-adherent particles across the model and human FAE

Our expression data suggested that our initial proposal to target β_1-integrin would indeed be a feasible strategy to improve uptake into human Peyer's patches. In addition to β_1-integrin, we identified an upregulation of the α_5- and α_8–integrin subunits on the mRNA level in the model

FAE (Fig. 2). Therefore, we chose a general integrin-targeting sequence in order to maximize adherence and the uptake and transport of nanoparticles. The RGD-peptide motif (Arg-Gly-Asp) is known to compete with *Yersinia* Invasin A in binding to β_1-integrin (Leong et al., 1995), but also to recognize many other integrins, including the α_5- and α_8-integrin subunits (Ruoslahti et al., 1996). CD9 also seemed promising, but to date, no ligands have been reported for human CD9. It was judged beyond the scope of this study to identify such molecules and thus we decided to study the effects of targeting integrins.

Optical sectioning of whole tissue specimens in a confocal microscope showed uptake of RGD-coated particles across the FAE as early as 15 minutes after application (Fig.6A). After 45 minutes, the RGD-coated particles had crossed the FAE and were found deep inside the dome (Fig.6B), while particles without peptide were not taken up at all (Fig. 6C). In the corresponding villus specimens, particles were mainly found associated with the luminal cell surface and inside epithelial cells at 15 minutes (Fig.6D). At 45 minutes, we could find RGD-particles also below the VE (Fig.6E), while particles without peptide were not taken up (Fig.6F). Uptake of both submicron-sized particles and aggregates of several microns were detected across both the FAE and VE. In addition, a large number of diffusely fluorescent, cellshaped bodies were found beneath the epithelium, suggesting that particles had been taken up by macrophages or dendritic cells (Fig 6 G,H). Thus, it was quite difficult to assess the magnitude of uptake with certainty. However, we could not at any time-point detect uptake of RGD-negative particles in either FAE or villus tissue (Fig.6C, F), while at 45 minutes, RGD-coated particles were found inside all the subepithelial domes of the PP and the villi studied (Fig, 6B,E).

To assess the specificity of the RGD-mediated uptake we performed transport experiments using particles coated with either RGD or RGE (Arg-Gly-Glu). In RGE, the aspartic acid,

15

which is most critical for integrin binding has been substituted with glutamic acid, which confers similar charge, but abolishes binding (Leong et al., 1995).

In our model FAE, the number of transported RGD-coated particles was 20-fold higher than particles coated with RGE (Fig.7, $p < 0.01$). There was no significant increase in transport of RGD-coated particles across the Caco-2 epithelium compared with RGE-coated particles. Preincubation of model FAE cell monolayers with soluble RGD (sRGD) significantly reduced the transport of RGD-coated particles.

In human ileal specimens, the transport of RGD-coated particles across the FAE and underlying tissue was 4-fold higher than the transport of RGE-coated particles (Fig. 8, $p < 0.001$). Surprisingly, RGD-coated particles were also transported across the VE. However, the transport of RGD-coated particles was 3-fold higher across the FAE than the VE ($p < 0.01$), while there was no difference in transport of RGE-coated particles across FAE and VE. sRGD significantly reduced the transport of both RGD- and RGE-coated particles across the FAE and VE ($p < 0.001$).

Discussion

So far, the human FAE has been sparsely studied with regard to markers and possible targets

for oral vaccines. In this study we have identified two surface-exposed cell adhesion

molecules, CD9 and β_1-integrin, with increased expression in human ileal FAE. Both are

potential targets for oral vaccine formulations. Furthermore, we provide quantitative data on

particle transport across the human intestinal mucosa. Our study shows that while the uptake

of plain nanoparticles across the intestinal wall is virtually undetectable, general targeting to

integrins results in a dramatically improved particle uptake. Thus, we show that it is possible

to use integrin targeting to enhance nanoparticle uptake into human Peyer's patches. To our

knowledge, our study is the first ever that provide data on targeting to the human FAE.

It is known that various integrins mediate, and potentially regulate, uptake of particulate

antigens in cell culture and animal studies (Kerr, 1999, Schulte et al., 2000). An earlier study

showed that β_1-integrin expressed apically on M-cells was responsible for the adherence and

uptake of *Yersinia* bacteria across the mouse FAE (Clark et al., 1998). Recently, Tyrer et al.

confirmed and extended this finding, by showing that β_1-integrin associates with α_5-integrin in

mediating integrin-dependent uptake of bacteria across mouse M-cells (Tyrer et al., 2006). In

our study, β_1-integrin stained the apical membranes of dome epithelial cells associated with

CD20-positive lymphocytes. Thus, the transport of RGD-coated particles across the FAE was

possibly mediated by M-cells. However, apical expression of β_1-integrin was occasionally

also found in dome epithelial cells not associated with CD20-positive lymphocytes and it

cannot be excluded that integrins expressed on other FAE cells contributed to the increased

uptake. The presence of integrins in human FAE has not been reported previously, but it is

known that their expression is tightly regulated (Lussier et al., 2000).

The tetraspan proteins, such as CD9, are known to modulate both the location and the

conformation of many proteins, including integrins, through binding and interactions within

17

so-called tetraspanin webs in the cell membrane (Berditchevski et al., 1999). Specifically, earlier studies have demonstrated an association between CD9 and β_1-integrin-precursors in epithelial cells (Rubinstein et al., 1997), suggesting that CD9 is involved in maturation and delivery of β_1-integrins to the cell membrane. CD9 has also been shown to play a role in protein kinase C-mediated integrin signalling (Zhang et al., 2001) and focal adhesion kinase-induced reorganisation of the cortical actin cytoskeleton (Berditchevski et al., 1999). Both of these events are critical for integrin-mediated uptake of particulate antigens (Dramsi and Cossart, 1998). Interestingly, a previous study also identified an mRNA transcript of a tetraspan protein (TM4SF3) with specific expression in the human FAE (Lo et al., 2004). Thus, CD9 and possibly other tetraspan proteins, may play a role in the regulation of integrin-mediated uptake.

Regardless of the tetraspan-interaction, the relationship between integrin expression levels and functionality was evident in this study. The median difference and variability in RGD-mediated nanoparticle transport between the FAE and the VE (Fig. 8), compares well with the mean difference and variability in β_1-integrin expression between the FAE and the VE (Fig. 5). Our transport data also clearly demonstrate the functional involvement of integrins in the particle uptake. There was a four-fold increase in transport between RGD- and RGE-coated particles across the FAE, which had an increased expression of β_1-integrins. However, no significant difference was found between RGD- and RGE-coated particles in VE, where we found no β_1-integrin expression. The involvement of other, co-expressed, RGD-binding integrins in the uptake can of course not be excluded. Their expression in human FAE is not known.

Since RGD and RGE induced nanoparticle transport across the VE to the same extent, it was conceivable that a mechanism other than integrin-interaction was of importance for this uptake. As hydrophobic latex particles coated with only the hydrophilic Pluronic linker were

not taken up at all (Fig. 6), we could exclude the involvement of an unspecific interaction

with the latex particle surface. Furthermore, we could not find any difference in particle size

or aggregation tendency between Pluronic-coated and peptide-Pluronic-coated particles

during our initial characterization studies (Andersson et al., 2005), which excluded a size

effect. Thus, the most likely explanation is a charge interaction between the peptide-coated

particles and the VE cells or mucus. Both RGD and RGE contain amino acids that confer both

positive (arginine) and negative charge (aspartic and glutamic acid) at pH 6-7.5, while the

Pluronic linker is uncharged in this pH range. Also, free RGD peptide inhibited both RGD-

and RGE-mediated uptake. In the FAE, however, the transport of RGD-coated particles was

much higher than the transport of RGE-coated particles. Judging from these data, the

contribution of charge to the improved transport across the FAE was less than 25%, indicating

that the specific interaction with integrins was of major importance (Fig. 8).

Our data certainly points to the necessity for a specific interaction when aiming at improved

uptake into Peyer's patches. Despite the improvement in nanoparticle transport seen with both

RGD and RGE, we did not find a significant difference in the uptake of RGE-coated particles

across the FAE compared with the VE. This further supports that the FAE mediated an

increased particle uptake by the specific expression of integrins and not by unspecific

mechanisms, such as an increased accessibility or a higher transport capacity. The difference

in CD9 expression levels between FAE and VE were even more prominent than for β_1-

integrin and it would be exciting to investigate the selectivity of a CD9 targeting sequence for

the human FAE, once a ligand has been discovered.

A possible application of our findings would be to improve the uptake of subunit oral vaccine

formulations. The crucial question is therefore, if the uptake of particles, even after targeting,

will be sufficient to initiate an immune response. Two hours after administration of RGD-

coated particles, 1 % of them had crossed the entire FAE and underlying tissue (Fig. 8). We

19

are not aware of any previous studies of intestinal particle transport across human tissues using the Ussing chamber technique and thus comparisons are difficult. However, our data can possibly be qualitatively compared with animal studies where particles have been instilled in ligated intestinal loops. From our confocal microscopy studies we approximate that at least 50 RGD-coated particles of sizes up to 5 µm was found in each dome covered by FAE after 45 minutes. During experiments with ligated loops in the mouse intestine, using cross-linked starch particles, only one to three particles (2 µm in size) were taken up in 4 out of the 10 studied domes after 45 minutes (Stertman, 2004). However, a lower dose of these particles than the one used in the loop initiated a prominent immune response after oral administration (Strindelius et al., 2002). The RGD-mediated uptake of 50 or more particles in our study was at least 20 times higher, but whether it will be sufficient to initiate an immune response after oral administration remains to be seen.

In conclusion, by using our recently introduced technique to obtain human FAE (Keita et al., 2006), we have been able to investigate the transport of nanoparticles into human Peyer's patches and assess the relative contribution of FAE and VE to nanoparticle uptake in the human intestine. We show that uptake of nanoparticles is a rare event, also in human intestine, but that the uptake into Peyer's patches may be dramatically improved by introducing an integrin targeting moiety on the particles. Apart from integrins, the integrin-associated cell adhesion molecule CD9 has an increased expression in human FAE and also holds as a potential target, once a targeting ligand has been identified. These findings provide a platform for improving the intestinal uptake and effects of oral vaccine formulations in humans.

JPET #107847

Acknowledgments

References

Andersson M, Fromell K, Gullberg E, Artursson P, Caldwell KD (2005) Characterization of surface-modified nanoparticles for *in vivo* biointeraction. A sedimentation field flow fractionation study. *Anal. Chem.* **77**:5488-5493.

Berditchevski F and Odintsova E (1999) Characterization of integrin-tetraspanin adhesion complexes: role of tetraspanins in integrin signaling. *J Cell Biol* **146**:477-492.

Brayden DJ (2001) Oral vaccination in man using antigens in particles: current status. *Eur J Pharm Sci* **14**:183-189.

Clark MA, Hirst BH and Jepson MA (1998) M-cell surface beta1 integrin expression and invasin-mediated targeting of Yersinia pseudotuberculosis to mouse Peyer's patch M cells. *Infect Immun* **66**:1237-1243.

Dalgleish AG, Beverley PC, Clapham PR Crawford DH, Greaves MF and Weiss RA (1984) The CD4 (T4) antigen is an essential component of the receptor for the AIDS retrovirus. *Nature* **312**:763-767.

des Rieux A, Ragnarsson EGE, Gullberg E, Preat V, Schneider YJ, Artursson P (2005) Transport of nanoparticles across an in vitro model of the human intestinal follicle associated epithelium. *Eur J Pharm Sci* **25**:455-465.

Dramsi S and Cossart P (1998) Intracellular pathogens and the actin cytoskeleton. *Annu Rev Cell Dev Biol* **14**:137-166.

Finzi G, Cornaggia M, Capella C, Fiocca R, Bosi F, Solcia E and Samloff IM (1993) Cathepsin E in follicle associated epithelium of intestine and tonsils: localization to M cells and possible role in antigen processing. *Histochemistry* **99**:201-211.

Foster N, Clark, MA, Jepson MA and Hirst B (1998) Ulex europaeus 1 lectin targets microspheres to mouse Peyer's patch M-cells in vivo. *Vaccine* **16**: 536-541.

Gebert A, Rothkötter H-J and Pabst R (1996) M cells in Peyer's patches of the intestine. *Int Rev Cytol* **167**:91-159.

Giannasca P, Giannasca K, Leichtner AM and Neutra MR (1999) Human intestinal M cells display the Sialyl Lewis A antigen. *Infect Immun* **67**:946-953.

Gullberg E, Leonard M, Karlsson J, Hopkins AM, Brayden D, Baird AW and Artursson P (2000) Expression of specific markers and particle transport in a new human intestinal M-cell model. *Biochem Biophys Res Commun* **279**:808-813.

Hamzaoui N, Kerneís, S, Caliot, E and Pringault, E (2004) Expression and distribution of beta 1 integrins in in vitro-induced M cells: implications for Yersinia adhesion to Peyer's patch epithelium. *Cell Microbiol* **6**: 817-828

Hussain N and Florence AT (1998) Utilizing bacterial mechanisms of epithelial cell entry: invasin-induced oral uptake of latex nanoparticles. *Pharm Res* **15**: 153-156.

Jepson MA, Clark MA, Foster N, Mason CM, Bennett MK, Simmons NL and Hirst BH (1996) Targeting to intestinal M-cells. *J Anat* **189**:507-516.

Keita Å, Gullberg E, Ericson A-C, Salim SY, Wallon C, Kald A, Artursson P, Söderholm JD (2006) Characterization of antigen and bacterial transport in the follicle-associated epithelium of human ileum. *Lab Invest* **86**:504-516

Kernéis S, Bogdanova A, Kraehenbuhl J-P and Pringault E (1997) Conversion by Peyer's patch lymphocytes of human enterocytes into M cells that transport bacteria. *Science* **277**:949-952.

Kerr JR (1999) Cell adhesion molecules in the pathogenesis of and host defence against microbial infection. *Mol Pathol* **52**:220-230.

Leong JM, Morrissey PE, Marra A and Isberg RR (1995) An aspartate residue of the Yersinia pseudotuberculosis invasin protein that is critical for integrin binding. *EMBO J* **14**:422-431

Lo D, Tynan W, Dickerson J, Scharf M, Cooper J, Byrne D, Brayden D, Higgins L, Evans C and O'Mahony DJ (2004) Cell culture modeling of specialized tissue: identification of genes expressed specifically by follicle-associated epithelium of Peyer's patch by expression profiling of Caco-2/Raji co-cultures. *Int Immunol* **16**:91-99.

Lussier C, Basora N, Bouatrouss Y, Beaulieu JF (2000) Integrins as mediators of epithelial-cell matrix interations in the human small intestinal mucosa. *Microsc Res Tech* **51**:169-178

Mantis N, Frey A and Neutra M (2000) Accessibility of glycolipid and oligosaccharide epitopes on rabbit villus and follicle-associated epithelium. *Am J Phys* **278**:G915-G923.

Mutwiri G, Bowersock TL and Babiuk LA (2005) Microparticles for oral delivery of vaccines. *Expert Opin Drug Deliv* **2**:791-806.

Neutra MR (1999) M cells in antigen sampling in mucosal tissues. *Curr Top Microbiol Immunol* **236**:17-32.

O'Hagan DT and Rappuoli R (2006) Novel approaches to pediatric vaccine delivery. *Adv Drug Deliv Rev* **58**:29-51

Owen RL (1999) Uptake and transport of intestinal macromolecules and microorganisms by M cells in Peyer's patches--a personal and historical perspective. *Semin Immunol* **11**:157-163.

Rubinstein E, Poindessous-Jazat V, Le Naour F, Billard M and Boucheix C (1997) CD9, but not other tetraspans, associates with the beta1 integrin precursor. *Eur J Immunol* **27**:1919-1927.

Ruoslahti E (1996) RGD and other recognition sequences for integrins. *Annu Rev Cell Dev Biol* **12**:697-715.

Russell-Jones GJ (2004) Use of targeting agents to increase uptake and localization of drugs to the intestinal epithelium. *J Drug Target* **12**:113-123.

Schulte R, Kerneis S, Klinke S, Bartels H, Preger S, Kraehenbuhl JP, Pringault E and Autenrieth IB (2000) Translocation of Yersinia entrocolitica across reconstituted intestinal epithelial monolayers is triggered by Yersinia invasin binding to beta1 integrins apically expressed on M-like cells. *Cell Microbiol* **2**:173-185.

Sharma R, van Damme EJM, Peumans WJ, Sarsfield P and Schumacher U (1996) Lectin binding reveals divergent carbohydrate expression in human and mouse Peyer's patches. *Histochem Cell Biol* **105**:459-465.

Sincock PM, Mayrhofer G and Ashman LK (1997) Localization of the transmembrane 4 superfamily (TM4SF) member PETA-3 (CD151) in normal human tissues: comparison with CD9, CD63, and alpha5beta1 integrin. *J Histochem Cytochem* **45**:515-525.

Smith MW, Thomas NW, Jenkins PG, Miller NG, Cremaschi D and Porta C (1995) Selective transport of microparticles across Peyer's patch follicle-associated M cells from mice and rats. *Exp Physiol* **80**:735-743.

Stertman L (2004) *Starch microparticles as an oral vaccine adjuvant with emphasis on the differentiation of the immune response*, Acta Universitatis Upsaliensis,Uppsala, Sweden.

Strindelius L, Degling-Wikingsson L and Sjoholm I (2002) Extracellular antigens from Salmonella enteritidis induce effective immune response in mice after oral vaccination. *Infect Immun* **70**:1434-1442.

Tyrer P, Foxwell AR, Cripps AW et al (2006) Microbial pattern recognition receptors mediate M-cell uptake of a gram-negative bacterium. *Infect Immun* **74**: 625-631.

van der Lubben IM, Verhoef JC, van Aelst AC, Borchard G and Junginger HE (2001) Chitosan microparticles for oral vaccination: preparation, characterization and preliminary in vivo uptake studies in murine Peyer's patches. *Biomaterials* **22**:687-694.

Wong NA, Herriot M and Rae F (2003) An immunohistochemical study and review of potential markers of human intestinal M cells. *Eur J Histochem* **47**:143-150.

Yamanaka T, Straumfors A, Morton H, Fausa O, Brandtzaeg P and Farstad I (2001) M cell pockets of human Peyer's patches are specialized extensions of germinal centers. *Eur J Immunol* **31**:107-117.

Zhang XA, Bontrager AL and Hemler ME (2001) Transmembrane-4 superfamily proteins associate with activated protein kinase C (PKC) and link PKC to specific beta(1) integrins. *J Biol Chem* **276**:25005-15013.

JPET #107847

Footnotes

b) Requests for reprints should be sent to: Professor Per Artursson, Dept. Pharmacy, Box 580, BMC, SE-751 23 Uppsala Sweden. Mail to: Per.Artursson@farmaci.uu.se, Phone: +46-18-471 4471

LEGENDS FOR FIGURES

Figure 1. Expression of β_1-integrin in human Peyer's patches. FAE: follicle-associated epithelium; VED: villus epithelium adjacent to dome and VE: villus epithelium. Where appropriate, stitched lines outline the surface of the epithelium. Boxes in A and B mark areas of magnification for C and D. **(A)** In the FAE, β_1-integrin was expressed on the basolateral membrane, or **(B)** in the entire plasma membrane of the epithelial cells. In the surrounding villi (VED/VE), it was predominantly expressed on the basal aspect of the epithelial cells and in the lamina propria. **(C, D)** Magnification of the FAE in (A) and (B) showed infiltration of CD20-positive lymphocytes into the epithelium (arrows). **(D, F)** At several sites, prominent apical expression of β_1-integrin was found in these lymphocyte-associated epithelial cells (arrows). **(E)** Apical expression of β_1-integrin was occasionally also found in FAE cells that were not associated with CD20-positive lymphocytes, but most commonly **(F)**, in FAE cells that were lymphocyte-associated (arrows).

Figure 2. Genes with changed expression in the model FAE compared with the Caco-2 epithelium. Gene names correspond to NCBI nomenclature and have been grouped according to reported functions. Shades of grey represent the ratio of gene expression in the model FAE compared with the Caco-2 epithelium (see legend).

Figure 3. Immunofluorescence of CD9, CD4 and β_1-integrin in the model FAE (A, C, E) and Caco-2 epithelium (B, D, F). Optical XZ-section of cell monolayers with the apical surface of the cells oriented upwards. Each image is representative of three independent experiments. Densitometric graphs of the corresponding fluorescence intensities are shown on the right side of each image. The expression of CD9 was higher in model FAE (**A**) than in the Caco-2 epithelium (**B**). CD4 expression was not detected in the model FAE (**C**) or the Caco-2

epithelium (**D**). The expression of β_1-integrin was higher in the model FAE (**E**) than in the Caco-2 epithelium (**F**) and found mainly on the apical cell surface of the model FAE. Bars indicate 10 µm.

Figure 4. Expression of CD9 in human Peyer's patches. FAE: Follicle-Associated Epithelium; VED: Villus Epithelium adjacent to Dome and VE: Villus Epithelium. Bars indicate 100 and 10 µm respectively. (**A**) CD9 was predominantly expressed in the FAE (arrows), while the VED showed little expression of CD9 (arrowhead). No or low expression of CD9 was found in the VE (arrowhead). However, CD9 expression was found on cells in both the lamina propria and the subepithelial dome region (arrowheads, magnification 16x). (**B**) Higher magnification (63 x) of the FAE showed that CD9 was expressed in the entire plasma membrane of the epithelial cells.

Figure 5. Quantification of CD9 and β_1-integrin expression in human Peyer´s patches from 8 individuals. (**A**) A section of ileal tissue demonstrating the three types of epithelia that were studied: follicle-associated epithelium (FAE), villus epithelium adjacent to dome (VED) and villus epithelium (VE). Four to eight sections were studied for each individual and each data point represents the mean fluorescence intensity of (**B**) CD9 or (**C**) β_1-integrin in one individual. See method section for details. Lines cross at the average fluorescence intensity of all patients and bars show the 95% confidence intervals. ***:$p<0,0001$; **: $p<0,01$; *: $p<0,05$, n.s.:, non-significant = $p>0.05$

Figure 6. Uptake of 200 nm RGD-coated (+RGD) and non-coated (-RGD) polystyrene particles in Peyer's patches and villus tissue. The images show optical XZ-sections of PP and villus tissue 15 and 45 minutes after addition of particles to the mucosa. Each timepoint is

illustrated by a representative fluorescent image (magnification 100x). F-actin-staining of

non-permeabilized tissues was used to visualize the epithelium (red). The epithelial cells

display green autofluorescence, while particles are seen in yellow, single or as aggregates.

The scalebar was used to assess the position of particles within the tissue (the epithelial cell

height was on average 20 µm). **(A)** In the FAE, the RGD-coated particles where found below

the epithelial cell layer already after 15 minutes **(B, C)** After 45 minutes, many of the

particles had crossed the FAE and were found in the subepithelial layer, while non-coated

particles had not been taken up at all. **(D)** In the VE, the RGD-coated particles were mainly

associated with the epithelium after 15 minutes, but after 45 minutes **(E)** particles could also

be detected beneath the VE. **(F)** Non-coated particles were not taken up at all across the VE.

(G,H) Diffusely fluorescent bodies beneath both FAE and VE probably represent cells that

have taken up particles (large arrows). Bars show 10 µm.

Figure 7. Transport of 200 nm RGD-coated (integrin-binding) and RGE-coated (non-integrin-binding) polystyrene particles across model FAE and Caco-2 epithelium.
Both model FAE and Caco-2 epithelium were preincubated with HBSS or soluble RGD-

peptide (sRGD) and the transported fluorescent particles measured by flow cytometry. Each

box shows median, interquartile range (25-75) and standard deviation of 8-24 filters, run on 3-

6 separate occasions. ****:** $p < 0.01$ for all groups compared with the transport of RGD-coated

particles across the model FAE.

Figure 8. Transport of 200 nm RGD-coated and RGE-coated polystyrene particles
across human Peyer's patches and villus tissue mounted in Ussing chambers. Both PP

and VE tissues were preincubated with Krebs buffer or soluble RGD-peptide (sRGD). The

number of particles found in the serosal buffer after 2 hours was assessed by flow cytometry

and is presented as the fraction of particles transported. This accounts for the difference in the

effective number of particles added to the mucosal chamber. Each box shows median,

interquartile range (25-75) and standard deviation of 3-5 separate measurements in 2

individuals. **: $p < 0.01$ or less for all groups compared with the transport of RGD-coated
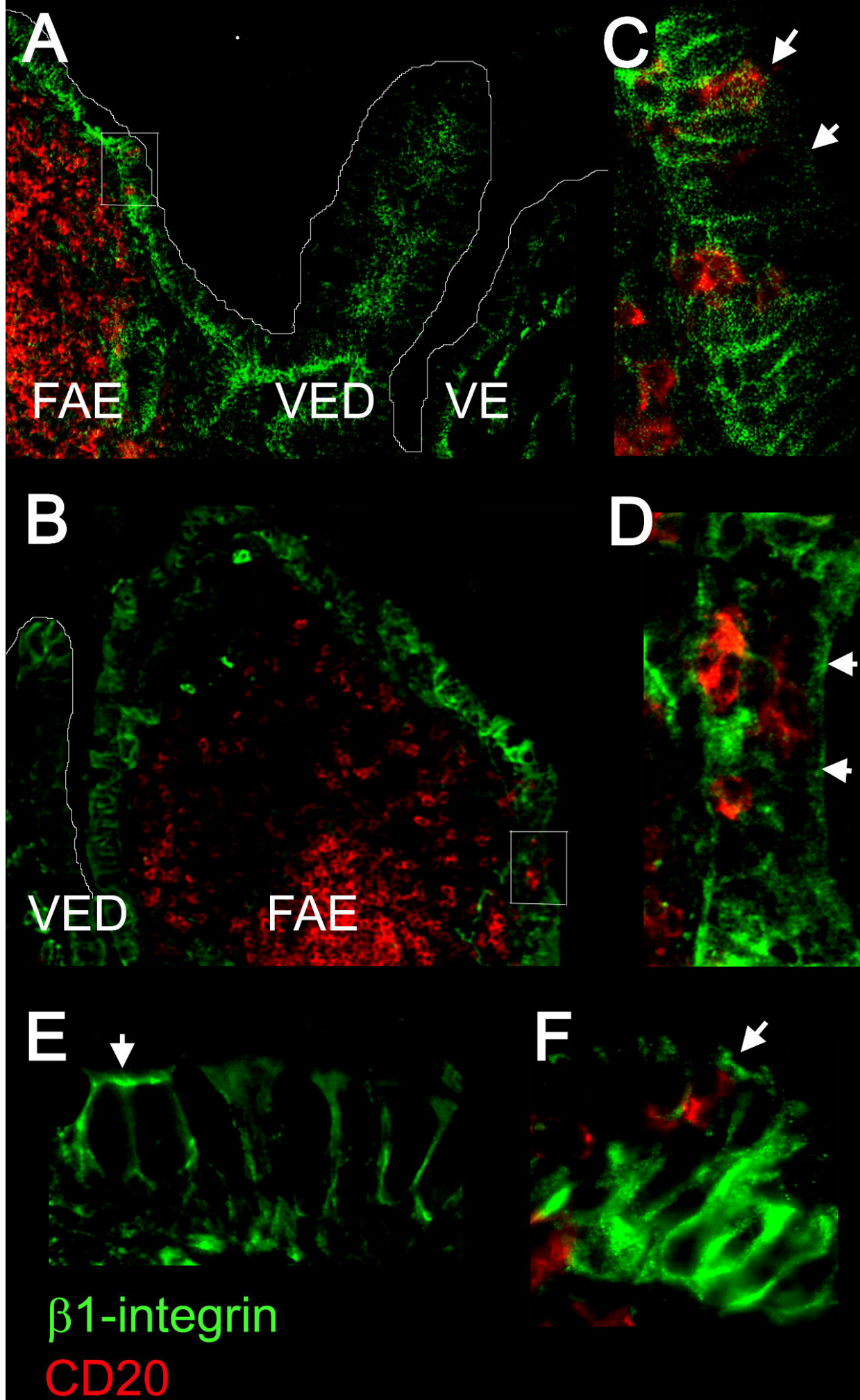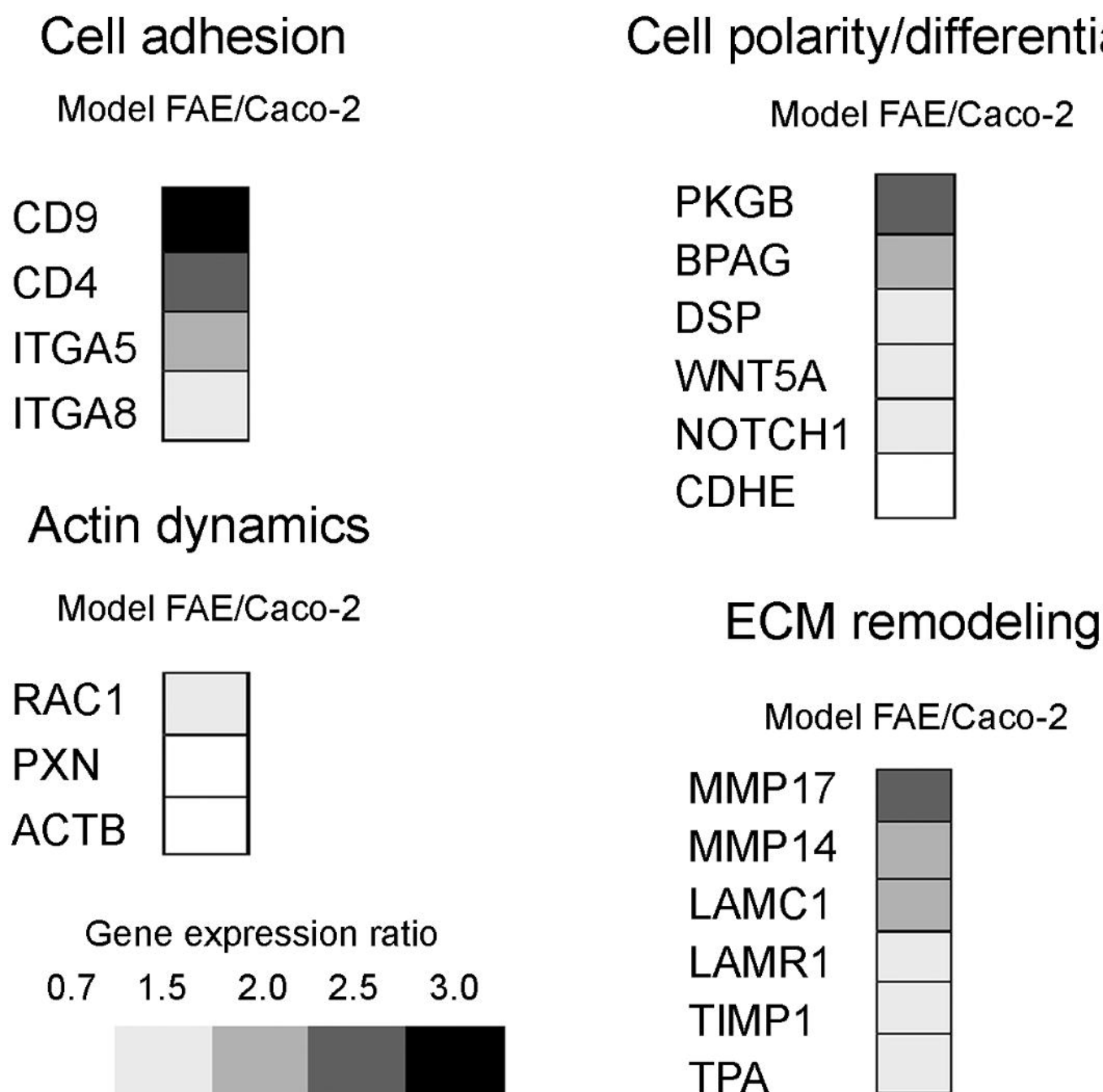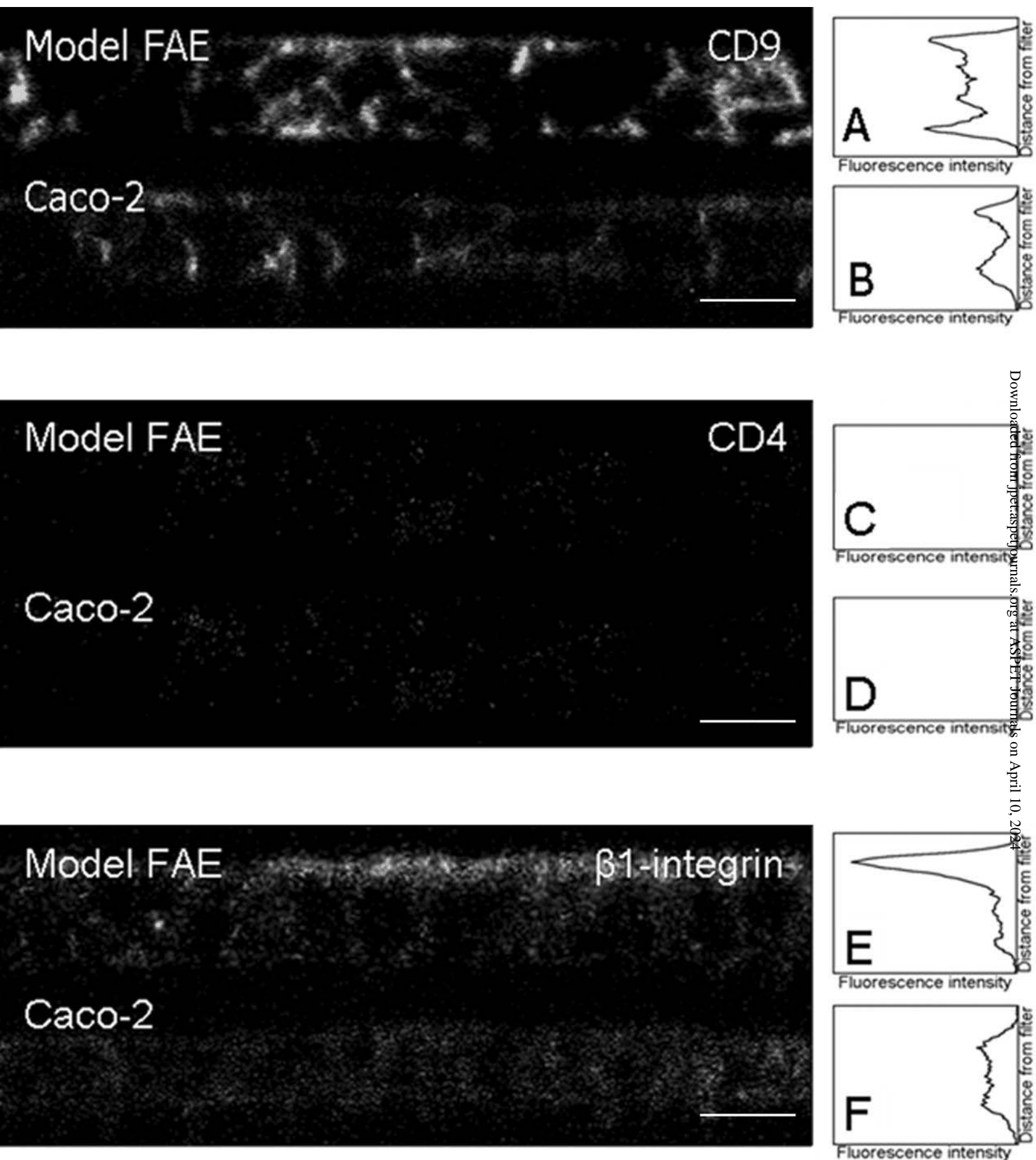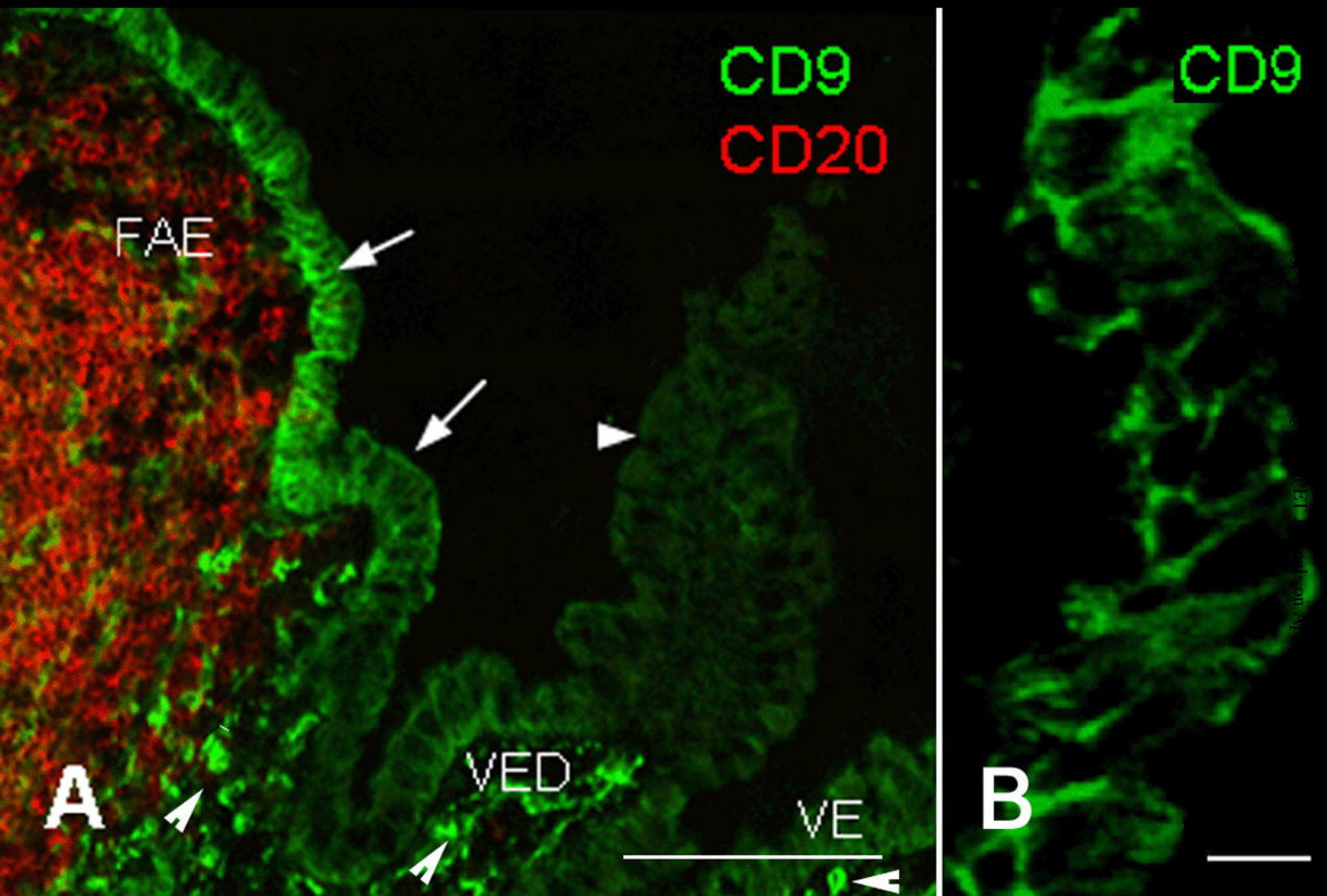
particles across the FAE.

Figure 1

A

FAE   VED   VE

B

VED   FAE

C

D

E

F

β1-integrin

CD20
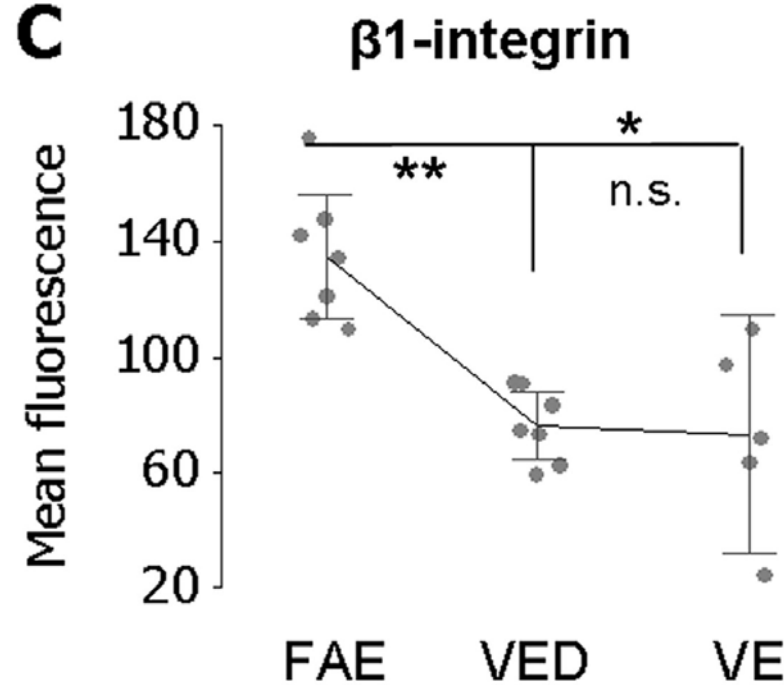
Figure 2

Figure 3

Figure 4

Figure 5

A

FAE   VED   VE

B

CD9

***

***

***

***

Mean fluorescence

180

140

100

60

20

FAE   VED   VE

C

β1-integrin

**

*

n.s.

Mean fluorescence

180

140

100

60

20

FAE   VED   VE
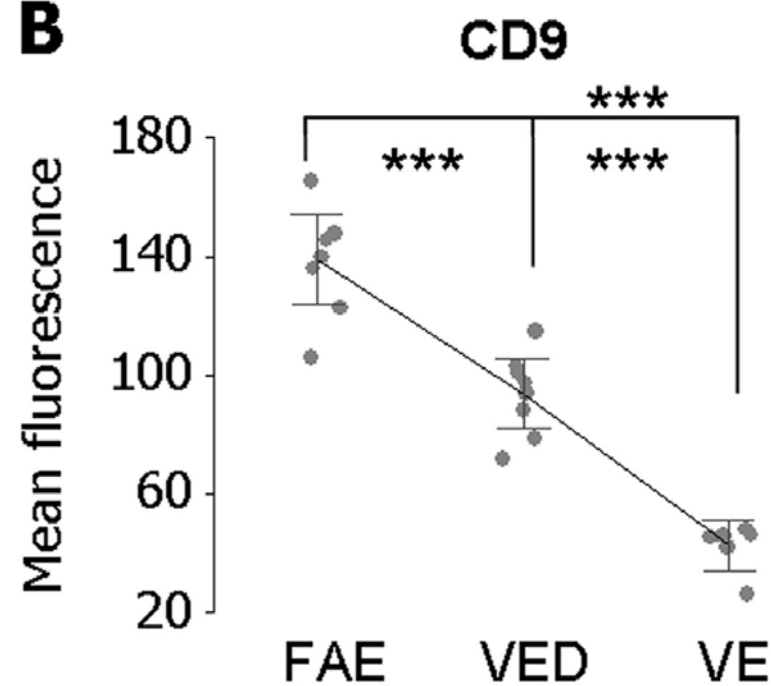
Figure 6

Figure 7

Figure 8